

Internal Report IASF-BO/CNR 365/2003

February 2003

**CONVERTING ECP MAPS TO HEALPix MAPS
WORKING IN REAL SPACE**

B. CAPPELLINI¹, C. BURIGANA² AND P. PLATANIA¹

Document: PL-LFI-IAFbo-MA-003

Revision: Issue 1.0; February 2003

Prepared by: Benedetta Cappellini, Carlo Burigana, Paola Platania

Authorized by: Fabio Pasian

¹*Dipartimento di Fisica, Università di Milano, via Celoria 16,
I-20133, Milano, Italy*

²*IASF/CNR, Sezione di Bologna, via P. Gobetti 101,
I-40129, Bologna, Italy*

Document: PL-LFI-IASFbo-MA-003

Revision: Issue 1.0; February 2003

Prepared by: Benedetta Cappellini, Carlo Burigana, Paola Platania

Authorized by: Fabio Pasian

Current code version: 1.0 - February 2003

Current code authors: Benedetta Cappellini, Carlo Burigana, Paola Platania

February 2003

Document: PL-LFI-IAFbo-MA-003

Revision: Issue 1.0; February 2003

CONVERTING ECP MAPS TO HEALPix MAPS WORKING IN REAL SPACE

B. CAPPELLINI¹, C. BURIGANA² AND P. PLATANIA¹

¹*Dipartimento di Fisica, Università di Milano, via Celoria 16, I-20133,
Milano, Italy*

²*IASF/CNR, Sezione di Bologna, via P. Gobetti 101, I-40129, Bologna, Italy*

SUMMARY - We present in this report a procedure to convert sky maps from a rectangular ECP pixelization of the sphere to the HEALPix scheme. The conversion is performed via an intermediate step, i.e. an intermediate HEALPix map possibly with a resolution higher than that desired for the final one. Criteria for the optimum intermediate resolution are discussed on the basis of numerical tests applied to very different kinds of sky maps.

1 Introduction

The Hierarchical Equal Area and iso-Latitude Pixelization of the sphere (HEALPix, Górski et al. 1999) is currently widely adopted in the astrophysical community and it has been chosen by the WMAP and PLANCK team to produce and release their CMB sky maps. It's therefore useful to provide tools able to convert maps with other pixelizations into the HEALPix scheme. We deal here with the conversion from the Equi Cylindrical Projection (ECP) pixelization, defined in Sect. 2, widely used in astronomical context.

The ideal situation to derive a sky map in a given pixelization is, of course, to project directly into a such map the Time Ordered Data of the considered experiment; in many circumstances, however, this approach is very difficult or even not possible. In principle, there are two ways to convert a map from a given pixelization to another one:

1. to work in Fourier space: compute the $a_{\ell,m}$ coefficients of the spherical decomposition from the original map, and then generate a map (with equal or lower resolution) with another pixelization.
2. to work in real space: to each pixel of the new pixelization scheme a proper signal value is assigned on the basis of the signal(s) in the corresponding pixel(s) of the original map.

We consider here the second approach that can be applied independently of the sky coverage and the kind of pixelisation of the original map.

The plan of this work is as follows. In Sect. 2 we describe our main assumptions and the proposed conversion procedure. In Sect. 3 we discuss the quality of the procedure applying the method to three representative cases. In Sect. 4 we summarize our findings and draw our conclusions. The code is described in Appendix A.

2 Method

The ECP pixelization is a rectangular projection of the sphere. For a full sky map, the ranges of the x (or φ) and y (or ϑ) axes are then 2π and π large respectively. The resolution parameter is N_φ , i.e. the number of pixels on the φ axis (usually $N_\varphi = 2^n, n \in \mathbb{N}$). The map is then stored in a $(N_\varphi, N_\varphi/2)$ matrix in φ and ϑ with dimensions $N_\varphi \times N_\varphi/2$. Sky coordinates are as follows: the longitude $\varphi \in [0, 2\pi)$ (anti-clockwise orientation) and the colatitude $\vartheta \in [0, \pi]$ (North–South orientation). More precisely the pixels centre of the considered ECP pixelisation are defined by:

$$(\vartheta, \varphi) = \left(\left(\frac{N_\varphi}{2} - j \right) \Delta + \frac{\Delta}{2}, \left(\frac{N_\varphi}{2} - i \right) \Delta + \frac{\Delta}{2} + 2\pi \cdot \left[\frac{i}{N_\varphi/2} \right] \right) \quad (1)$$

where $i \in [1, N_\varphi]$, $j \in [1, N_\varphi/2]$, $\Delta = 2\pi/N_\varphi$ is the angular dimension of the ECP pixels and $[a]$ is the integer part of the real number a .

The HEALPix¹ pixelization is a curvilinear partition of the sphere. The resolution parameter is N_{side} , i.e. the number of divisions along the side of the 12 base-resolution pixels (it has to be $N_{\text{side}} = 2^x, x \in [0, 13]$). The total number of pixels for a map is $N_{\text{pixHEALPix}} = 12 \cdot N_{\text{side}}^2$. All pixels have identical area, and their centers are distributed along lines of constant latitude. These geometrical properties makes HEALPix a powerful discretization of the sphere for accurate statistical and astrophysical analyses of high resolution data sets.

Given the ECP map resolution N_φ , the corresponding HEALPix N_{side} parameter is such that $N_{\text{pixECP}} \sim N_{\text{pixHEALPix}}$. In practice, given the limitations on the parameters values, this relations reads $N_{\text{side}} \sim N_\varphi/4$.

Anyway, it is possible to perform the pixelization conversion with a higher HEALPix resolution and then degrade the map to the final one. We think that in this way the different orientation of corresponding pixels in the two pixelizations will have a minor impact on the HEALPix final map: we so expect that the best choice for the intermediate step of the procedure is the map with the higher N_{side} .

In the following we refer to the final resolution with $N_{\text{side_fin}}$ and to the intermediate resolution with $N_{\text{side_interm}}$.

The code acts in this simple way: given the $N_{\text{side_interm}}$ value, for every HEALPix pixel the code finds the corresponding ECP pixel (see Appendix A for details) and assigns its signal value. The map is finally degraded to $N_{\text{side_fin}}$.

To test the procedure, we compute the conversion with all the $N_{\text{side_interm}}$ equal or higher than $N_{\text{side_fin}}$, which are computationally available within the HEALPix routines². Final results are, as expected, not identical: we must define criteria to determine the optimum $N_{\text{side_interm}}$ for a given $N_{\text{side_fin}}$.

We considered the following data set:

¹For a detailed description of HEALPix concept, routines and parameters, refer to the HEALPix documentation available at <http://www.eso.org/science/healpix>.

²Due to high memory request, we only run the code up to $N_{\text{side_interm}} = 4096$.

1. the HEALPix maps with a fixed $N_{\text{side_fin}}$, obtained with different values of $N_{\text{side_interm}}$.
2. the relative differences of such maps with “adjacent” $N_{\text{side_interm}}$ HEALPix parameters (e.g. comparing results obtained by using $N_{\text{side_interm}} = 256$ and 512).

In the first case we compute the mean, variance, Kurtosis and Skewness, plus the peaks ratio. In the second case we compute mean, rms values, and the number of pixels with relative difference higher than 1%.

We will study the convergence of these estimators, to determine the optimum choice of $N_{\text{side_interm}}$.

3 Case study

We applied the method to a plenty of cases, both real and synthetic maps with different spatial signatures; we show here results for three representative cases (in these examples $N_\varphi=1024$ and $N_{\text{side_fin}}=256$).

1. A publicly available³ low frequency sky map (Haslam et al. 1982), after destriping (Platania et al. 2003); it represents a “real” case distribution.
2. A synthetic map with spiraling signal

$$\text{signal}(i, j) = j + (i - 1)/N_\varphi$$

with $i \in [1, N_\varphi]$, $j \in [1, N_\varphi/2]$. Note that the distribution of the values (i.e. the number of pixels assuming a given value) for such a map is perfectly flat and symmetric.

3. A synthetic map with a random Gaussian distribution of values, i.e. a “noisy” map (we report results for such a distribution with r.m.s. = 150).

The statistical moments of the resulting HEALPix maps are shown in Table 1 and 2. In Table 1 the statistical moments are also reported for the ECP maps for a comparison.

In the first two cases, the same behaviour of the map statistical moments for increasing $N_{\text{side_interm}}$ is found, and, looking also at Table 2 (particularly evident in the last two columns), there is a clear evidence that increasing $N_{\text{side_interm}}$ the statistical moments of the resulting HEALPix maps tend to converge to stable values.

Variance, Skewness and Kurtosis of an ECP map are quite different from the corresponding HEALPix maps values since, for a non-equal area pixelization map, the moments evaluated in this simple way do not have a well defined meaning. To verify this “geometrical” interpretation, we created a testing map doubling the polar caps in the HEALPix map with the higher $N_{\text{side_interm}}$: a rectangular projection has more pixels near the poles than on the equator to cover the same area on the sky, and doubling the polar caps is a simple way to reduce this discrepancy. In Table 1 we show results considering twice pixels with colatitude $\vartheta \in [0, 40^\circ] \cup [140^\circ, 180^\circ]$.

For the Haslam map, the Skewness and Kurtosis indices approach the ECP values, confirming our hypothesis. Mean and variance do not have significant variations, but this is due to the proper distribution of the signal in the map (e.g. the map is in ecliptic coordinates: the considered doubled North polar cap contains a fraction of the Galactic plane with the highest values, and in fact the mean is increased).

³<http://skyview.gsfc.nasa.gov>

For the spiralizing map, as expected, the r.m.s and Kurtosis approach the ECP values, while the mean is not affected at all (in fact, we double symmetric values of the map with respect to the mean, which thus is not changed) and the Skewness index maintains a very small value, since the distribution is still symmetric.

In the third case (the “noisy” map with no coherent structure), the convergency of the procedure, not particularly evident from the results in Table 2, is again probed by the results reported in Table 1. Note that the HEALPix map with $N_{\text{side_interm}} = 256$ has moments rather different from the others HEALPix maps and very similar to those of the ECP input map. In fact, in this case there is a relation nearly 1 to 1 among the pixels of the two schemes ($N_{\text{pix_HEALPix_interm}} \sim N_{\text{pix_ECP}}$) and the Gaussian distribution is then sampled in a similar way in the two schemes.

For the Gaussian map, none of the moments has a significant variation after doubling the polar caps. This can be understood by considering the distribution of the values in the map. In fact, the polar caps contain – as the whole map – randomly Gaussian distributed numbers, so the new map has the same Gaussian distribution as the one without doubled caps. In this case, the performed test does not help to understand the discrepancy in the ECP–HEALPix moments and is not reported (as discussed above, the HEALPix map with $N_{\text{pix_HEALPix_interm}} \sim N_{\text{pix_ECP}}$ shows in this case statistical moments most close to those of the ECP input map).

The ratio between the maximum values of the map in the two different schemes is in general a decreasing function of $N_{\text{side_interm}}$. This is because pixels with signal higher than the nearest ones are sampled and averaged in a different way by working at different intermediate resolution. In fact, this effect is negligible in the spiral map (which has a complete plain signal) and can reach a level of $\simeq 15\%$ in the case of the “noisy” map, where the signals of adjacent pixels are completely uncorrelated. Of course, this effect is related to the intrinsic differences between the two pixelization schemes.

Anyway, this effect is of the order of a few % in the case of maps of diffuse Galactic-like components.

Finally, to further support the method, in the case of the Haslam map, we compute the ratio between the differences of the HEALPix maps with adjacent $N_{\text{side_interm}}$ and the sensitivity of the Haslam map (~ 7.42 K in $N_{\text{side}} = 256$ HEALPix pixels). Results are shown in Table 3; we compute mean, r.m.s., plus the percentage of pixels with absolute values of this ratio smaller than 0.01 and larger than 1 (clearly, the “conversion” uncertainty on the pixel value in the HEALPix map is negligible in the error budget if this ratio is much smaller than 1 for the majority of the pixels). Again, as expected, there is a clear improvement of the result for increasing $N_{\text{side_interm}}$.

We have verified that the same conclusions apply also to other maps, not shown here, for which the signal distribution has a behaviour similar to those described in this report, which represent quite general classes of sky map spatial distributions.

As an example, the Haslam map in ECP and HEALPix pixelization ($N_{\text{side_interm}} = 4096$) is shown in Fig. 1 (rectangular projection) and Fig. 2 (mollweide projection), respectively.

4 Conclusions

We implemented a simple method to convert sky maps from a rectangular ECP pixelization of the sphere into the HEALPix scheme. The method works in the real space and can be applied independently of the input map sky coverage. The method makes use of an

intermediate HEALPix map, with an higher N_{side} parameter than desired for the final map. We tested the procedure to optimise the final HEALPix map properties, i.e. to choose the optimum N_{side_interm} value. The performed tests show that the procedure is solid, and the best strategy for the conversion is to make use of the highest available value of N_{side_interm} .

Acknowledgements. Some of the results in this paper have been derived using the HEALPix (Górski et al. 1999).

References

- [1] Górski, K.M., Hivon, E., Wandelt, B.D., 1999, “Proceedings of the MPA/ESO Conference on Evolution of Large-Scale Structure: from Recombination to Garching”, ed. Banday A.J., Sheth R.K., Da Costa L., pg. 37, astro-ph/9812350
- [2] Haslam, C.G.T., Stoffel, H., Salter, C.J., Wilson, W.E., 1982, A&AS, 47, 1
- [3] Platania, P., Caserini, E., Maino, D., Burigana, C., Bersanelli, M., Cappellini, B., Men-
nella, A., 2003, A&A, submitted, astro-ph/0303031

A The code

Authors: B. Cappellini, C. Burigana, P. Platania.

The tool is provided as a `module`.

The conversion subroutine can be called with a file or an array as ECP input data.

In the first case, ECP maps are supposed to be in FITS format. In the output FITS file, the header reports the original header plus parameters on the conversion procedure.

Installation of `cfitsio` library is a prerequisite.

ECP_TO_HEALPIX.f90

FORMAT

call `ecp_to_healpix(filename_ecp, nphi_ecp, filename_he, nside_he, nside_interm, ordering, costconv)`

or

call `ecp_to_healpix(data_ecp, nphi_ecp, data_he, nside_he, nside_interm, ordering, costconv)`

ARGUMENTS

name	description
<code>filename_ecp</code> (or <code>data_ecp</code>)	the input ECP map file the input ecp map array)
<code>nphi_ecp</code>	ECP resolution of the input map
<code>filename_he</code> (or <code>data_he</code>)	the output HEALPix map file the output HEALPix map array)
<code>nside_he</code>	HEALPix resolution of the output map
<code>nside_interm</code>	HEALPix intermediate resolution
<code>ordering</code>	final map can be stored both in ‘nested’ or ‘ring’ scheme.
<code>costconv</code>	a numerical value, to change, if necessary, the data units.

INTERNAL SUBROUTINES:

- `ReadMap`

A routine to call the proper reading routine⁴, depending of the input file type. Both binary tables or arrays can be read.

- `vec_iphijth_ecp`

This is the “core” of the conversion procedure: given the HEALPix pixel spherical coordinates (ϑ, φ) it finds the corresponding ECP pixel:

$$(\vartheta, \varphi) \rightarrow (i, j) = (\text{int}((2\pi - \varphi)/\Delta)) + N_\varphi/2 + 1, (\text{int}((\pi - \vartheta)/\Delta) + 1)$$

where $i \in [1, N_\varphi]$, $j \in [1, N_\varphi/2]$ and $\Delta = 2\pi/N_\varphi$ is the angular dimension of the ECP pixels.

⁴From the `FitsMod` module, see the `MODULES&ROUTINES` section below.

MODULES&ROUTINES

This section lists the external modules and routines used by ecp_to_healpix.

module name	routine or function name
- HEALPix modules and routines	
healpix_types	—
udgrade_nr	udgrade_nest
pix_tools	pix2vec_nest
	convert_nest2ring
bit_manipulation	
num_rec	
-PLANCK BBM modules and routines	
fitsMod	ReadArray
	ReadBintab
	WriteFullSky
	pushHeader
	headerLine

Table 1: Statistics for maps projected into HEALPix scheme.

#	N_{side} interm	mean	variance	Skewness index	Kurtosis index	max(HEALPix)/ max(ECP)
HASLAM MAP						
HEALPix	256	34.7924	1576.29	17.5739	1023.74	1.0000
	512	34.8093	1604.97	18.2684	1049.52	0.9997
	1024	34.8081	1588.71	17.3915	951.855	0.9997
	2048	34.8062	1581.12	17.0211	908.536	0.9890
	4096	34.8082	1593.67	17.0540	908.836	0.9815
	4096 [‡]	35.0773	1593.62	20.8748	1278.86	
ECP		33.5721	1424.82	24.8547	1819.68	
SPIRAL MAP						
HEALPix	256	256.972	12408.7	7.72412×10^{-4}	-0.805140	0.999758
	512	256.999	12410.5	9.54379×10^{-6}	-0.805791	0.999758
	1024	256.993	12410.6	1.67630×10^{-4}	-0.805804	0.999758
	2048	256.991	12410.1	2.24121×10^{-4}	-0.805682	0.999758
	4096	256.990	12410.1	2.30252×10^{-4}	-0.805682	0.999758
	4096 [‡]	257.029	16390.7	-6.91807×10^{-4}	-1.12086	
ECP		256.999	21842.9	3.19413×10^{-6}	-1.20004	
GAUSSIAN MAP						
HEALPix	256	-0.309527	22465.3	-0.00909653	0.00951052	1.00000
	512	-0.253775	14040.3	-0.0101967	0.454405	0.868199
	1024	-0.253532	12550.6	-0.0113430	0.559142	0.848408
	2048	-0.280366	12244.2	-0.0111300	0.596552	0.839888
	4096	-0.277075	12172.8	-0.0110578	0.604392	0.844607
	ECP		-0.266859	22479.9	-0.00456042	0.0149348

[‡]HEALPix map with doubled polar caps 40° high. See the text for more details (Sect. 3).

Table 2: Statistics for relative differences of HEALPix maps with adjacent $N_{\text{side_interm}}$.

	mean value	r.m.s.	N (> 1%)
HASLAM MAP			
(map512-map256)/map256	3.10273×10^{-4}	0.0179519	8.54632
(map512-map256)/map512	1.13920×10^{-4}	0.0128478	8.42870
(map1024-map512)/map512	4.53056×10^{-4}	0.00574412	1.68737
(map1024-map512)/map1024	1.54656×10^{-5}	0.00532600	1.65329
(map2048-map1024)/map1024	7.22982×10^{-6}	0.00240654	0.298055
(map2048-map1024)/map2048	1.48943×10^{-6}	0.00238987	0.290807
(map4096-map2048)/map2048	1.06626×10^{-5}	0.00110417	0.0509898
(map4096-map2048)/map4096	9.44855×10^{-6}	0.00109914	0.0499725
SPIRAL MAP			
(map512-map256)/map256	-1.34064×10^{-5}	1.63222×10^{-3}	0.174459
(map512-map256)/map512	-1.60987×10^{-5}	1.64999×10^{-3}	0.168610
(map1024-map512)/map512	1.87781×10^{-6}	7.21364×10^{-4}	0.0394185
(map1024-map512)/map1024	1.35394×10^{-6}	7.26505×10^{-4}	0.0372569
(map2048-map1024)/map1024	3.11551×10^{-6}	3.42946×10^{-4}	0.00508626
(map2048-map1024)/map2048	2.99767×10^{-6}	3.43496×10^{-4}	0.00508626
(map4096-map2048)/map2048	5.08517×10^{-7}	1.69821×10^{-4}	0.00101725
(map4096-map2048)/map4096	4.79708×10^{-7}	1.69729×10^{-4}	0.00101725
GAUSSIAN MAP			
(map512-map256)/map256	-0.108517	255.623	16.6860
(map512-map256)/map512	-0.654459	405.613	29.6234
(map1024-map512)/map512	0.012259	205.395	31.1373
(map1024-map512)/map1024	0.482053	564.259	37.7565
(map2048-map1024)/map1024	0.315301	297.810	37.4377
(map2048-map1024)/map2048	0.101013	59.3366	40.4986
(map4096-map2048)/map2048	0.0556647	38.7630	36.2719
(map4096-map2048)/map4096	-0.0886737	150.106	37.6063

Table 3: Haslam map. Statistics for differences of HEALPix maps with adjacent $N_{\text{side_interm}}$ with respect to the sensitivity of the observations.

	mean value	r.m.s.	N (< 0.01)	N (> 1)
HASLAM MAP				
(map512-map256)/sens.	2.0×10^{-3}	0.63	75.15	0.25
(map1024-map512)/sens.	-5.8×10^{-5}	0.25	85.74	0.07
(map2048-map1024)/sens.	-3.6×10^{-4}	0.11	93.95	0.014
(map4096-map2048)/sens.	2.3×10^{-4}	0.04	97.34	0.009

The destriped Haslam map in ECP (Fig. 1) and HEALPix (Fig. 2) pixelization. The maximum value is limited to 300 in both cases (real maximum is ~ 4200) to see details of the maps.

Figure 1: Haslam map at 408 MHz in ECP pixelization. $N_\varphi=1024$.

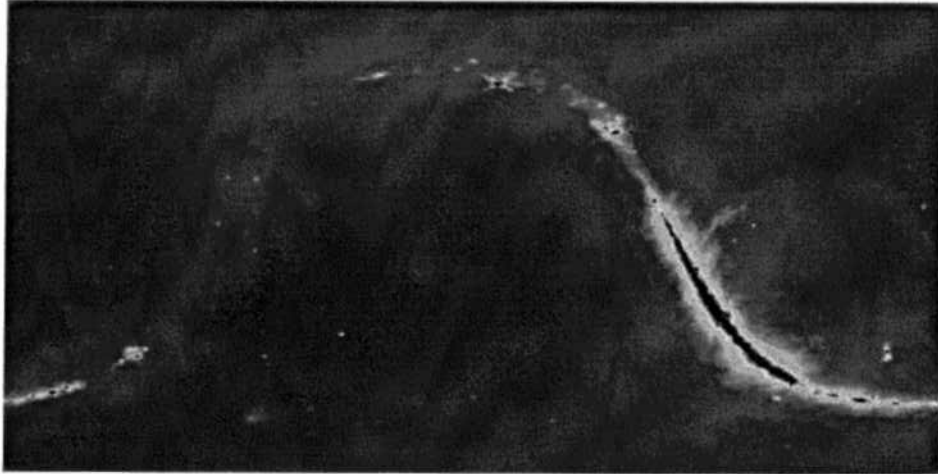


Figure 2: Haslam map at 408 MHz in HEALPix pixelization. $N_{\text{side}} = 256$.

